EDRAAK

Vol. **(2024)**, 2024, **pp**. 59–77
ISSN: 3078-8412

Research Article

Multi-view Deep Learning-Based COVID-19 Diagnosis with Chest X-Ray Images: A Comparative Study of SVM and KNN Classifiers

Hind abud-allah[1,*],

[1] *Islamic University Of Lebanon*

ARTICLE INFO

Article History
Received 25 Mar 2024
Revised: 20 May 2024
Accepted 20 Jun 2024
Published 5 Jul 2024

Keywords
Deep Learning,
Transfer Learning,
Feature Extraction,
Multi-View Classification,
SVM.

ABSTRACT

This study focuses on the detection of COVID-19 using chest X-ray images. With the rapid global spread of the highly contagious disease, early and accurate detection is crucial to prevent further transmission. We propose a multi-view approach that leverages different deep-learning methods to detect COVID-19 based on chest X-ray images. The framework presented in this study aims to capture both complementary and correlative information from multiple views. By using pre-trained deep convolutional neural network (CNN) models such as ResNet50 and VGG16 to extract deep features from the X-ray images. Support Vector Machine (SVM) and K-Nearest Neighbors (KNN) algorithms are then employed to classify the X-ray images based on the learned feature representations. The single-view models using VGG16 and ResNet50 with SVM achieved accuracy scores of 97% and 98% respectively. Similarly, using KNN, the single-view models achieved accuracy scores of 89% and 95%. Recognizing the potential of multi-view learning to improve generalization performance. We utilized early fusion to integrate the outputs of the pre-trained models and fed them into SVM and KNN classifiers. The multi-view model achieved accuracy scores of 98% and 92% respectively. The experimental results demonstrate that the multi-view deep learning methods outperformed the single-view deep models in detecting COVID-19 from chest X-ray images. The findings of this study have practical implications as they can assist experts in early diagnosis of COVID-19 cases, highlighting the effectiveness of the proposed methods.

1. INTRODUCTION

Covid disease, caused by the SARS virus, appeared in the city of Wuhan at the end of 2019, where it spread rapidly around the world, leading to pandemic [1]. The spread of the virus was through respiratory droplets, affecting more than 200 countries [2]. Until mid-2020, More than 4 and a half million cases of Coronavirus infection were recorded, and the total deaths are more than 300,000 people [8]. Symptoms can range from mild to severe, and some lead to pneumonia and respiratory distress syndrome as a result of this disease [3]. Governments and global health organizations have taken all considerations to mitigate the spread of the disease, including social distancing, vaccination campaigns [4][5]. However, health care systems faced major challenges due to the large number of cases and limited resources [6][7].
To address these challenges, this thesis aims to utilize deep learning techniques for predicting coronavirus infections. The availability of electronic health data provides an opportunity to train the machine and deep learning algorithms to improve disease prediction [8][9]. Within the framework of COVID-19, multi-view classification with deep learning entails categorizing several perspectives of chest X-ray pictures into distinct groups, including normal, COVID-19, and viral pneumonia. Deep learning algorithms may be used to detect patterns and characteristics in medical photos that may not be easily noticeable to humans.
Multi-view classification improves classification accuracy by integrating information from many perspectives or viewpoints of the same image. This methodology shows potential for precise and prompt identification of COVID-19, assisting in the endeavors to manage the disease. This study utilized a dataset including around 10,000 X-ray scans. Different methods were utilized to determine the proportion of lung damage in persons who are healthy compared to those who are sick. The support vector machine (SVM) technique demonstrated superior accuracy in digital image processing when compared to the k-nearest neighbors (KNN) and multi-view approaches. In addition, SVM exhibited a quicker picture processing time in comparison to alternative methods.
This work emphasizes the significance of employing deep learning techniques for multi-view categorization of COVID-19 pictures. It possesses the capacity to augment the velocity and precision of COVID-19 diagnosis, resulting in enhanced treatment and preventative approaches.

*Corresponding author email: h.abudallah1986@gmail.com
DOI: https://doi.org/10.70470/EDRAAK/2024/009

2. METHODOLOGY

This chapter discusses the methods used in carrying out the study. The aim of this study is to run a different Multiview deep learning algorithm to classify Multiview chest x-ray images into three different classes. The dataset used were carefully selected and processed to create datasets that suit the Vgg16 and Resnet50 pre-trained models. The machine's computational capacity was considered when choosing the model, the amount of data, and the training options. Support Vector Machines (SVMs) and K-Nearest Neighbors (KNN) are the classifiers selected for this thesis; we have also applied multi-view classification by using early fusion models.

2.1 Problem Statement

The problem statement for the Multi-view Classification of COVID-19 Images The purpose of using deep learning is to develop a fast, low-cost, and reliable method for automatic detection of COVID-19 based on radiological imaging of patients. Specifically, the study aims to use chest X-ray images to detect COVID-19, as they are cost-effective, have low ionizing radiation exposure to patients, and are widely available in hospitals. The proposed method utilizes a multi-view feature learning framework that extracts useful information from different views of the same image to learn more comprehensive feature representation for the diagnosis of COVID-19. The study uses a dataset consisting of COVID-19, normal, and pneumonia chest X-ray images, with the aim of achieving high accuracy scores in detecting COVID-19 cases.

2.2 Aim of the study

The objective of the study for Multi-view Classification of COVID-19 Images Using Deep Learning is to develop a reliable and accurate method for automatic detection of COVID-19 based on radiological imaging of patients. Specifically, the study aims to use chest X-ray images to detect COVID-19, as they are widely available in hospitals, cost-effective, and low ionizing radiation exposure to patients. The proposed method utilizes a multi-view feature learning framework that extracts useful information from different views of the same image to learn more comprehensive feature representation for the diagnosis of COVID-19. The study uses a dataset consisting of COVID-19, normal, and pneumonia chest X-ray images, with the aim of achieving high accuracy scores in detecting COVID-19 cases. The proposed approach aims to provide a fast, low-cost, and accurate solution to aid medical professionals in diagnosing COVID-19 and reducing the spread of the disease.

2.3 Block Diagram:

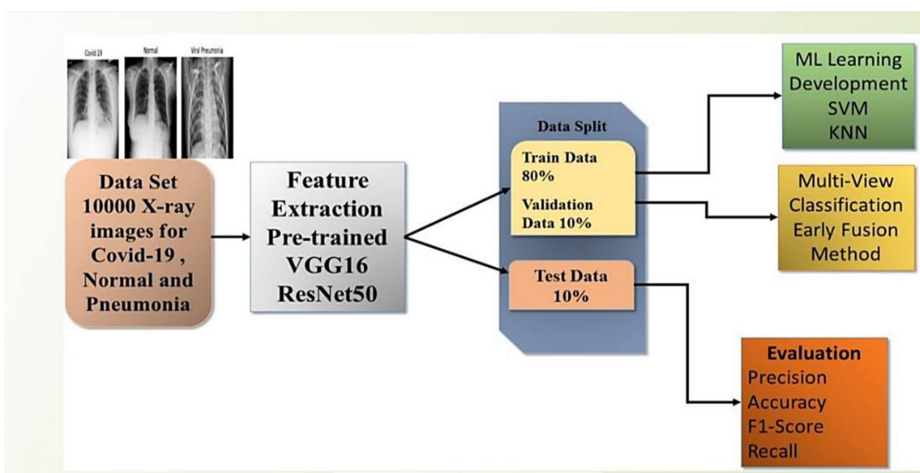

Fig 1: Project Diagram

The framework diagram of the specific context can be described as follows:

1. Dataset: The study uses a dataset of 10,000 X-ray images, which are divided into three categories: COVID-19, normal pneumonia, and viral pneumonia.
2. Extraction of features: The study uses two pre-trained deep learning models, VGG16 and ResNet50, to extract features from X-ray images. These models were trained on large datasets of natural images and learned to extract useful features that could be used for various computer vision tasks.
3. Data Segmentation: The data set is divided into three parts: training data (80%), validation data (10%), and test data (10%). The training data is used to train the machine learning models, the verification data is used to adjust the super parameters of the models, and the test data is used to evaluate the performance of the models.
4. Developing Machine Learning: The study uses two machine learning models, SVM and KNN, to classify X-ray images based on features extracted using VGG16 and ResNet50.

5. Multi-Display Classification: The study uses a multi-display classification approach, where X-ray images are divided into different views, and features are extracted from each view using VGG16 and ResNet50. These features are then combined using the early integration method, where the features are connected to form a single feature vector.
6. Evaluation: The performance of machine learning models is evaluated using various metrics such as accuracy, accuracy, F1 score, and recall.

Overall, the block diagram illustrates the different steps involved in the study, from data collection to model evaluation, for the automatic detection of COVID-19 using X-ray images and deep learning techniques.

2.4 Dataset description

The dataset used in this study consists of chest X-rays. Images were collected from two sources: the Kaggle COVID-19 radiography database [10] and chest X-ray images (pneumonia) [11].

The dataset was divided into three groups as shown in Figure (2): COVID-19, normal pneumonia, and viral pneumonia. These groups were created to be compatible with the pre-trained CNN used in the study and to help achieve the objectives of the study.

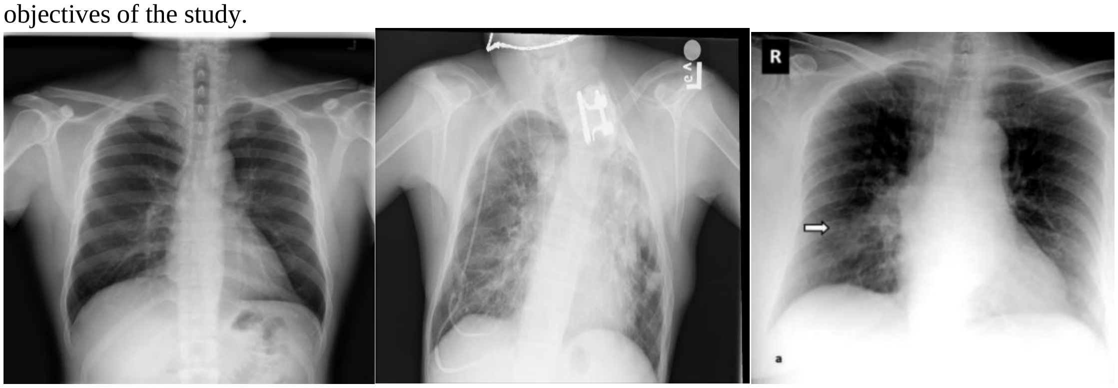

Fig 2: Normal images of viral pneumonia and COVID-19 from left to right respectively [12]

Methods for dividing a dataset into training and testing groups include allocating one part to the training of the model and another to evaluate its performance. A common practice is to split 80-20, with 80% used for training and the remaining 20% for testing and validation. However, the exact partitioning can be modified based on the size of the dataset and the specific use case. It should be noted that the dataset is balanced, indicating an almost even distribution of samples across both groups. Table (I) provides details on the distribution of balanced chest X-ray datasets.

TABLE I: DISTRIBUTION OF BALANCED CHEST X-RAY DATASETS

Split Type	**Training set 80%**	**validation set 10%**	**Testing set (Elec. Eng.) 10%**	**Total 100%**
natural	2640	330	330	3300
COVID-19	2640	330	330	3300
Viral Pneumonia: 6	2640	330	330	3300
Total	7,920	990	990	9900

- programing language

Python is a high-level, localized programming language widely used in a variety of applications, including scientific computing, data analysis, web development, and artificial intelligence/machine learning. It has become one of the most popular programming languages in recent years due to its ease of use and readability and the large number of libraries and frameworks available.

Overall, choosing Python 3 to process X-ray images using deep learning models such as VGG16, ResNet50, and Early Fusion was probably a smart decision, as it provides a powerful, efficient, and flexible platform for this type of work.

2.5 Python Software Environment

We used Anaconda and Jupyter to implement our model, because the data volume is too large on a PC with a 64-bit window, 16GB RAM, and 1.99GHzIntel® CoreTMi7-8550U CPU.

Python is a high-level programming language that is effective for public use. It supports multiple models. It has a large standard library that provides appropriate tools for performing various tasks. It's a simple, less clustered language with extensive features and libraries. Different programming abilities are used to perform the experiment in our work. In this study, the following Python libraries were used.

- Panda: A powerful data processing and analysis tool in Python, it has become a standard library in the data science community due to its efficiency and versatility.
- NumPy: A core library for numerical computing in Python, NumPy provides a versatile array object and a rich set of mathematical functions. It forms the backbone of many science and data analysis libraries and is widely used in various fields, including data science, machine learning, physics, and engineering.
- Matplotlib: Matplotlib is a popular Python library for creating visualizations and conspiracies. Provides a wide range of functions and tools to create high-quality charts, charts, histograms, scatterplots, and more. The Matplotlib library is highly flexible and customizable, allowing users to create post-quality visualizations for different purposes.
- TensorFlow: is a popular open-source Python library used for machine learning and deep learning applications. Provides a comprehensive ecosystem of tools, libraries, and resources to efficiently build and deploy machine learning models.
- Sklearn: is a popular Python library for machine learning and data analysis. Provides a wide range of algorithms, tools, and utilities for various machine learning tasks, including classification, regression, aggregation, dimensional reduction, model evaluation, and data pre-processing.

2.6 Pre-processing of datasets:

In deep learning methods, there is a standard procedure that involves pre-processing or disinfection of data. The primary objective of this phase is to prepare the data for use by the deep learning model, which facilitates smoother analysis and computational processing. Depending on the issue being addressed and the characteristics of the dataset available, some adjustments need to be made before submitting images to the deep learning model.

Image processing involves various tasks such as resizing, and may involve geometric shifts, color adjustments, grayscale shifting, and a myriad of other processes, depending on the nature of the problem and the characteristics of the dataset. In our study, we use some tasks such as normalizing the pixel values of images to have zero mean and unit contrast, and noise removal are noise reduction techniques such as Gaussian opacity or intermediate filtering that can be applied to reduce noise in images and remove duplicates that remove duplicate images from the dataset using a hash function that identifies files with identical binary content.

After the image pre-processing phase, we used the feature extraction method to capture relevant characteristics from the images, to serve as input to the deep learning model. This process involves extracting features related to texture, shape, and density from images.

After the feature is extracted, the dataset is usually respectfully divided into training, validation, and testing groups (80%, 10%, 10%). The training kit is used to train the deep learning model, while the validation kit is used to adjust the excessive parameters and prevent over-installation. Finally, the test set is used to evaluate model performance on invisible data.

In general, the goal of image processing and dataset preparation is to create a high-quality dataset that can be used to train an accurate and robust deep learning model for image classification tasks.

2.7 Implementation of Feature Extraction Techniques:

At this stage of implementation, we used two deep pre-trained models, VGG16 and ResNet50, to extract a range of features from chest X-rays. To get rid of the classification task, we froze the VGG16 layers up to a dense layer. By setting up top = false, we effectively removed the fully connected layers of the previously tested VGG16 model. The output from the VGG16 layer was a shape matrix (sample size, 7-7-512). We performed a similar analysis using the ResNet50 model by configuring it with pre-trained weights of “imagenet” and excluding the upper layers, with input form (224 - 224 - 3). Next, we fed the outputs from VGG16 and ResNet50 into two classifiers, SVM and KNN classifiers, for further analysis.

3. CLASSIFICATION METHODS

In this study, we used two approaches to categorization: single view categorization and multiple view categorization. The main concepts of these approaches are outlined below.

3.1 Classification of one offer:

In image categorization tasks, single-width categorization involves using only pixel values of images as input features, without considering additional information such as image metadata or context. Similarly, in the taxonomy of a text, the taxonomy of a single presentation entails the analysis of the content of the text alone, ignoring any supplementary information.

Single-width classification methods rely solely on features extracted from the point of view chosen to make predictions. These methods are often easy to implement and interpret, making them suitable for various applications. However, they may not make full use of all available information, especially in complex datasets where multiple perspectives can provide complementary insights.

3.1.1 Integration of SVM with VGG16 and ResNet50:

SVM is a supervised learning algorithm used for classification, regression, and extreme detection. They work by finding the super-optimal level that separates data into different categories based on their features. As mentioned earlier, ResNet50 and VGG16 were used to extract features. |||UNTRANSLATED_CONTENT_START|||SVM It is a supervised learning algorithm used for classification, regression, and outlier detection. |||UNTRANSLATED_CONTENT_END||| They work by finding the super-optimal level that separates data into different categories based on their features. As mentioned earlier, ResNet50 and VGG16 were used to extract the feature.

Our work can be summarized by the following key steps. First, we collected a dataset of X-ray images that include normal chest conditions, COVID-19, and viral pneumonia, which were appropriately labeled. To assess the performance of our models, the dataset was divided into training and testing sets. The training group was used to train the model, while the testing group worked on evaluating the performance of the model. To prepare the images for analysis, we applied pretreatment techniques. This involved resizing images to a uniform size, normalizing pixel values, and converting them to either grayscale or RGB, depending on the specific requirements of the models used.

Next, we fed pre-processed images through both VGG and ResNet50 individually to extract their respective feature offerings. This step allowed us to capture the distinctive characteristics and patterns present in the images. Next, we trained the SVM classifier using the features extracted from the images in the previous step. The SVM model was trained on the training set, leveraging the extracted features to learn the distinctive features between the different chest states.

To evaluate the performance of the SVM model, we used the test set and calculated several key matrices, including accuracy, accuracy, recall, and F1 score. These matrices provided insights into the model's ability to accurately classify chest conditions in the test group.

Furthermore, we conducted a comparative analysis of the performance of the SVM model when combined with both VGG16 and ResNet50 models. We evaluated the accuracy and other relevant matrix to determine which model achieved superior results. Overall, these steps formed the core components of our work, enabling us to classify chest X-ray images using single view and multiple view approaches.

3.1.2 Integration of KNN with VGG16 and ResNet50:

In our thesis, we expanded our analysis by incorporating a KNN classifier to evaluate features extracted from the VGG16 and ResNet50 models. The following steps have been taken to conduct this investigation.

Initially, we collected and categorized the datasets, which were later broken down into training and testing sets. Prior to the analysis, the images underwent pre-processing procedures to ensure consistency and improve their suitability for further processing. The pre-processed images were then passed through both CNN's pre-trained VGG16 and ResNet50 models, enabling relevant features to be extracted from each model. This step allowed us to capture important visual patterns and distinctive characteristics present in the images.

Next, we trained the KNN model using the features extracted from the images obtained in the previous steps. The training set was used to facilitate the learning process, enabling the model to identify patterns and make accurate classifications based on the extracted features. To evaluate the performance of the KNN model, we used the test set and calculated a different matrix such as accuracy, accuracy, recall, and f1 score. These matrices served as valuable indicators of the model's ability to accurately classify chest conditions within the test population.

Furthermore, we conducted a comparative analysis to evaluate the performance of the KNN model when combined with the features extracted from both the VGG16 and ResNet50 models. We used accuracy and other relevant matrix to identify the model that achieved superior results in this context.

By incorporating the KNN classifier into our analysis, we expanded our investigation to include the evaluation of feature extraction from VGG16 and ResNet50 models, further enhancing the comprehensiveness of our study.

3.1.3 Multi-Vision Classification:

To enhance classification performance in this thesis, a multi-view approach was implemented. The integration of the features extracted from the VGG16 and ResNet50 models was achieved through the introduction of early integration technology.

To start, deep features were extracted from both VGG16 and ResNet50 models for each input sample. These extracted features included diverse aspects and representations of the data, leading to a thorough understanding of the inputs.

Later, features extracted from both models were combined using an early integration approach. This merger aims to leverage the complementary information each model captures, resulting in a rich and more comprehensive representation of features.

After the merger, the fused features obtained were used as inputs for training SVM and KNN classifiers. These classifiers were specifically selected for their effectiveness in handling multilayered classification tasks.
By integrating features extracted from multiple views and training classifiers on the built-in features, the proposed multi-display approach aims to improve both classification accuracy and system robustness. This methodology provided a more comprehensive analysis by looking at different perspectives and leveraging the strengths of both VGG16 and ResNet50.

3.2 Performance Evaluation.

When evaluating the performance of a classification model for three categories, several scales can be used to assess how well the model is performing across different aspects. We use some common matrices [13]:

3.2.1 Confusion Matrix:

To deal with the problem of classification with three categories, a confusion matrix is needed to evaluate the performance of the models. The Confusion Matrix is a table showing the actual and expected categories for a set of situations.
For the three-category classification problem as in Figure (3) below, the confusion matrix is a 3x3 matrix that includes the following four scales:
- True Positive (TP): The model correctly predicted positive categories.
- False positive (FP): The model predicted the positive category, but the actual category was negative.
- True Negative (TN): The model correctly predicted the negative category.
- False Negative (FN): The model predicted the negative category, but the actual category was positive.

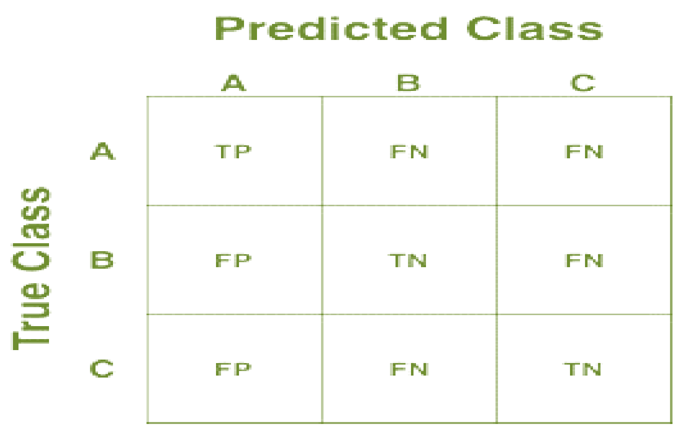

Fig 3: Confusion matrix for three categories [14]

Based on these metrics, we can calculate a different matrix to evaluate the performance of the classification model, including accuracy, recall, and f1 score, for each category individually, or we can calculate a weighted average across all categories.

3.2.2 Accuracy

Accuracy is a commonly used metric for evaluating the performance of classification models. Measures the proportion of correctly classified cases out of the total number of cases.
Specifically, accuracy is calculated as follows in Formula (1):

$$\text{Accuracy} = \frac{TP_A + TP_B + TP_C}{(TP_A + TP_B + TP_C \ + \ TN_A + TN_B + TN_C \ + \ FP_A + FP_B + FP_C \ + \ FN_A + FN_B + FN_C)} \quad (1).$$

For example, if a workbook classifies 90 out of 100 cases correctly, its accuracy will be:
Accuracy = 90/100 = 0.9 or 90%
While accuracy is a useful metric, it is important to note that it may not be the most appropriate metric for all classification tasks, especially in situations where categories are out of balance. In such cases, other matrix such as accuracy, recall, and F1 score may be more helpful. In addition, accuracy does not take into account the costs of misclassification, which may be important in some applications. For example, if the accuracy is 90% and the F1 score is 50%, the exact value should be neglected because it has many true negative value points. Therefore, it is important to consider the specific context and objectives of the rating task when selecting the appropriate performance measure.

3.2.3 Accuracy

In the context of confusion matrices, accuracy is a measure of the accuracy of positive predictions made by a classification model. It is defined as the ratio of true positive predictions to the total number of positive predictions made by the model.
More formally, accuracy is calculated as shown in Formula (2):

$$Precision = \frac{TP_A + TP_B + TP_C}{(TP_A + TP_B + TP_C) + (FP_A + FP_B + FP_C)} \quad (2).$$

Accuracy is a useful measure in cases where the cost of false positives is high, such as in medical diagnosis or fraud detection. High accuracy means the model makes fewer false-positive predictions, reducing the risk of false alarms or unnecessary interventions.
However, accuracy must be evaluated in conjunction with another matrix, such as recall and score f1, to obtain a complete picture of the performance of the classification model.

3.2.4 Summoning

Recall is a measure of confusion used to evaluate the performance of a rating model. It measures the proportion of actual positive cases (i.e., cases belonging to the positive category) that the model correctly identifies as positive.
The invocation formula appears in the formula (3):

$$\text{Recall} = \frac{TP_A + TP_B + TP_C}{(TP_A + TP_B + TP_C) + (FN_A + FN_B + FN_C)} \quad (3).$$

In other words, recall refers to the model's ability to identify all positive states, and a higher recall score means that the model is better at detecting positive states. However, a high recall score may come at the expense of a lower accuracy score (i.e., the model's ability to identify only positive states correctly). Therefore, it is important to consider both recall and accuracy when evaluating the classification model.

3.2.5 F1 – Outcome

A f1 score is a measure used to evaluate the performance of a rating model. It combines the accuracy and recall matrix into a single score representing the harmonic mean of the scale. The f1 score is often used when we want to balance accuracy and recall and we want both matrices to be considered equally important.
The form of the score of f1 is as shown in Formula (4)

$$\text{F1} - \text{score} = \frac{2(TP_A + TP_B + TP_C)}{2((TP_A + TP_B + TP_C) + (FP_A + FP_B + FP_C) + (FN_A + FN_B + FN_C))} \quad (4).$$

In other words, the f1 score is a measure of the accuracy of the model, taking into account both false positives (FP) and false negatives (FN). A higher f1 score indicates better performance of the rating model, a maximum score of 1 indicates perfect accuracy and recall, and a minimum score of 0 indicates poor performance. It should be noted that a score of f1 is more useful than accuracy when the categories are unbalanced, that is, when the number of cases in each category is uneven. In such cases, accuracy can be misleading, as a high degree of accuracy can be achieved simply by predicting the majority category in all cases. On the other hand, the f1 score takes into account the accuracy and recall of each individual class, providing a more accurate measure of model performance.

4. RESULTSAND DISCUSSION

This section focuses on the implementation and evaluation of different models for testing and classifying chest X-ray images into different groups. Discusses the performance of different proposed models and compares their results in different scenarios. The evaluation process in this thesis involves comparing different classification techniques. Specifically, we study the performance of single-width classification methods such as vector support machines (SVM) and k-Nearest Neighbors (KNN), which are tested on characteristic vectors extracted from our dataset. To achieve this, each deep feature extractor is used to create a distinct display that corresponds to our image dataset. In addition, we explore the effectiveness of multi-view ranking using an early integration approach. By ranking the single view, we evaluate the performance of the SVM and KNN algorithms individually, taking into account their feature vectors. This allows us to assess how well these technologies are performing when applied to our dataset.
Furthermore, we investigate multi-view ranking through the use of early fusion technology. This involves combining feature vectors extracted from different views or perspectives of the data. By combining information captured from multiple views, we aim to enhance classification accuracy and get more robust results. By comparing the results of a

single offer rating with a multiple offer rating using early integration, we gain insights into the benefits and limitations of each approach. This evaluation process helps us determine the most appropriate technique for the specific dataset and classification task.

4.1 Single Vision Classification Results:

As we review the results of the single vision ranking, we see how the two rankings performed.

4.1.1 SVM Workbook Results:

After applying the SVM classifier, the results of the classification process were analyzed. We found that the SVM classifier showed high accuracy rates for chest X-ray classification. Specifically, when we applied the SVM classifier to the features extracted from the ResNet50 model, it achieved an accuracy of 0.98. Similarly, when we applied the SVM classifier to the features extracted from the VGG16 model, it achieved an accuracy of 0.97. These high resolution rates indicate the durability and reliability of the SVM classifier in distinguishing different types of chest conditions or abnormalities in X-ray images.

4.1.1.1 SVM Workbook Results with ResNet50 Extracted Features:

Figure (4) represents the mixing matrix of the SVM classifier with features extracted from the ResNet50 model to classify three categories: COVID-19, normal pneumonia, and viral. The Confusion Matrix provides an overview of the workbook's performance by showing the number of cases that have been correctly or incorrectly classified for each category

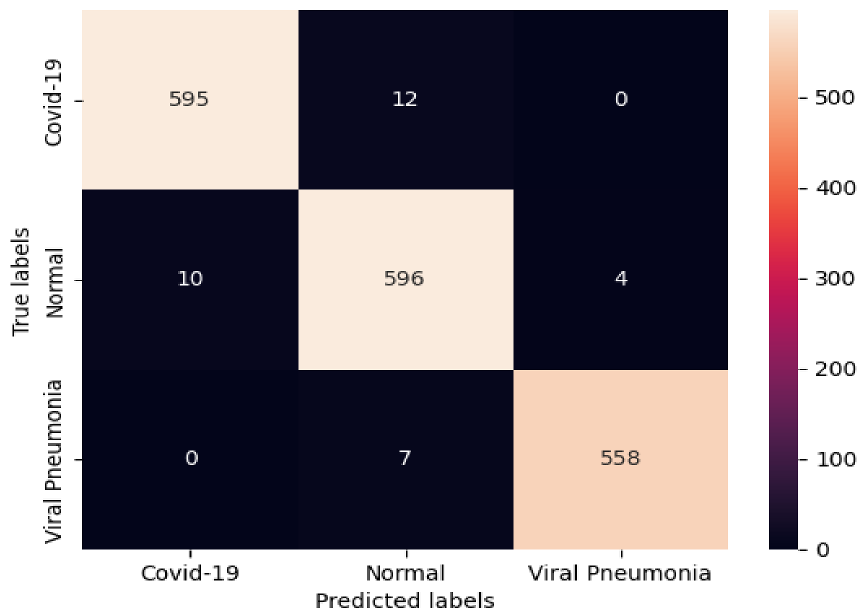

Fig 4: Confusion matrix for SVM classifier with features extracted using ResNet50 model.

The rows of the confusion matrix represent the real categories, while the columns represent the expected categories. In Grade 1, which corresponds to the COVID-19 category, there are a total of 607 cases. Of these cases, 595 were correctly classified as COVID-19 by an SVM classifier. I misclassified 12 cases as normal, but there were no cases incorrectly classified as viral pneumonia. Moving to the second row, which represents the normal category, there are 610 cases in total. She correctly classified 596 cases as normal, while she misclassified 10 cases as COVID-19 and 4 cases as viral pneumonia. Finally, in the last row, which represents the category of viral pneumonia, there are 565 cases. The SVM classifier correctly classified 558 cases as viral pneumonia. I misclassified 7 cases as normal, but there were no cases incorrectly classified as COVID-19.

Tables [2] in the study show the recall and result rates f1 and accuracy for each of our individual datasets. The values presented in these tables provide a detailed analysis of the performance of the proposed classification system based on the SVM classifier.

According to Table [II], the SVM classifier achieved an accuracy rate of 98%. Accuracy is a measure that indicates the proportion of correctly classified positive cases out of all cases classified as positive. In this case, it means that given chest X-rays rated as positive by the SVM classifier with ResNet50, 98% were correctly rated as positive.

Moreover, the table also shows a recall rate of 98%. Summoning, also known as sensitivity or true positive rate, measures the proportion of actual positive cases correctly identified by the classifier. In this context, he indicates that the SVM classifier correctly identified 98% of positive chest X-ray images.
Also, Table [II] indicates an f1 score rate of 98%. A f1 score rate of 98% indicates that the SVM classifier struck a high balance between correctly categorizing positive cases (accuracy) and correctly identifying all positive cases (recall).
Overall, these results show the strong performance of the SVM classifier along with the features extracted from ResNet50 in the classification of chest X-ray images, as evidenced by high resolution and recall rates and a f1 score of 98%.

TABLE II: SVM CLASSIFIER RESULTS WITH FEATURES EXTRACTED USING THE RESNET50 MODEL.

• **ResNet50**			
Fitness	Fig. 1. **Precision**	Fig. 2. **Recall**	Fig. 3. **F1 Score**
natural	0.97	0.98	0.97
Viral Pneumonia: 6	0.99	0.99	0.99
COVID-19	0.98	0.98	0.98
Moderate	0.98	0.98	0.98
Accuracy	Fig. 4. **0.98**		

4.1.1.2 Results of SVM Workbook with VGG16 Extracted Features:

Figure (5) below represents the confusion matrix of the SVM classifier with the features extracted from the VGG16 model to classify three categories: COVID-19, natural pneumonia and viral. Provides a summary of the workbook's performance by showing the number of cases that have been correctly or incorrectly classified for each category.
Looking at the matrix, we can see that the rows represent the real categories, while the columns represent the expected categories. In the first grade, we have a COVID-19 class. Out of a total of 607 COVID-19 cases, the classifier correctly classified 592 cases as COVID-19, while 14 cases were incorrectly classified as normal and 1 case as viral pneumonia. Moving to the second row, which represents the normal category, out of a total of 610 normal cases, the classifier correctly classified 592 cases as normal. However, I have misclassified 13 cases as COVID-19 and 5 cases as viral pneumonia.
Finally, in the last row, representing the viral pneumonia category, out of a total of 565 cases, the correctly classified 557 cases were classified as viral pneumonia. I have misclassified 1 case as COVID-19 and 7 cases as normal. High numbers on the diagonal of the matrix indicate good performance in classifying cases correctly for each category. However, out-of-country items show false classifications, indicating areas where the classifier may struggle to distinguish between certain categories.

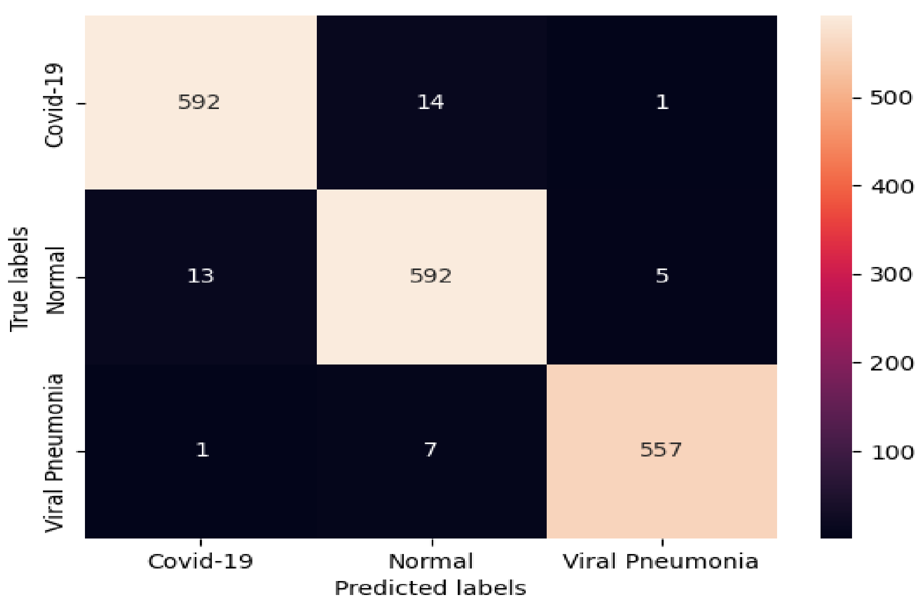

Fig 5: Confusion matrix for SVM classifier with features extracted using VGG16 model.

Table [III] shows the results of the SVM workbook when combined with the features extracted using the VGG16 model. The table shows the accuracy, recall, and f1 score matrix for each chapter, as well as average values across all chapters and overall accuracy.
For the normal category, the SVM classifier achieved an accuracy of 0.97, indicating that the samples classified as normal were indeed correctly classified. The recall value indicates that the workbook has determined an accuracy of 0.96 from the actual normal samples. The score of f1, which combines accuracy and recall, is 0.96, indicating a balanced performance between accuracy and recall for the normal category.
Similarly, for the viral pneumonia category, the SVM classifier achieved high accuracy and recall scores of 0.98 and 0.99, respectively. This indicates that the classifier was good at correctly identifying viral pneumonia samples. A f1 score of 0.99 also confirms the accuracy of the classifier for this class.
In the case of the COVID-19 category, the SVM classifier achieved an accuracy of 0.97, indicating that the samples were classified as COVID-19. A recall value of 0.98 indicates that the workbook has effectively identified actual COVID-19 samples. The f1 score of 0.97 reflects the overall performance of the classifier for this category.
The middle grade provides average accuracy, recall, and f1 score across all categories. In this case, the average accuracy and recall is 0.97, indicating consistent performance across all categories. The total resolution, shown separately, is 0.97, indicating a high level of accuracy for the SVM classifier with features extracted using the VGG16 model.
Overall, these results demonstrate the effectiveness of the SVM classifier in accurately classifying chest X-ray images of the studied categories when using features extracted from the VGG16 model.

TABLE III: SVM CLASSIFIER RESULTS WITH FEATURES EXTRACTED USING VGG16 MODEL.

• **VGG16)**			
• **Fitness**	[1] **Precision**	[2] **Recall**	[3] **F1 Score**
• **natural**	• 0.97	• 0.96	• 0.96
• **Viral Pneumonia: 6**	• 0.98	• 0.99	• 0.99
• **COVID-19**	• 0.97	• 0.98	• 0.97
• **Moderate**	• 0.97	• 0.98	• 0.97
• **Accuracy**	[4] **0.97**		

4.1.2 KNN Workbook Results:

We also applied the KNN classifier to features extracted from pre-trained CNN ResNet50 and VGG16. The results show that for chest X-ray classification, the KNN classifier produced an accuracy of 0.89 and 0.95 when using the VGG16 and ResNet50 models, respectively.

4.1.2.1 SVM Workbook Results with ResNet50 Extracted Features:

Figure (6) represents a confusion matrix resulting from the application of the KNN classifier to the features extracted using the ResNet50 model for three categories: COVID-19, normal pneumonia, and viral. The matrix provides valuable insights into classifier performance by depicting the number of correctly and incorrectly classified samples within each category.
Starting with the category “COVID-19”, the matrix reveals that out of a total of 577 samples belonging to this category, 577 samples were correctly classified as COVID-19. However, there were 28 cases in which samples from other categories were mistakenly classified as COVID-19, and two samples from the COVID-19 category were mistakenly classified as normal or viral pneumonia.
Moving to the “normal” category, there were 560 samples accurately classified as normal, while 42 samples from this category were incorrectly classified as COVID-19. In addition, 8 samples of the viral pneumonia category were mistakenly identified as normal.
In the case of the category “viral pneumonia”, the confusion matrix shows that out of 550 samples belonging to this category, 550 samples were correctly identified. However, there were 13 cases in which samples from other categories were incorrectly classified as viral pneumonia, and two samples from the viral pneumonia category were incorrectly assigned to either COVID-19 or the normal category.

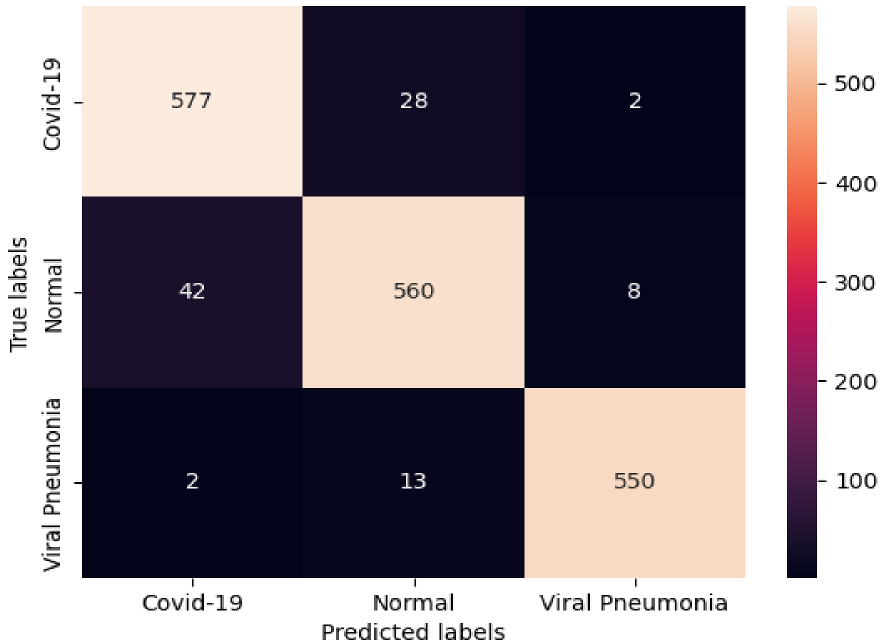

Fig 6: Confusion Matrix Forknn Classifier With Features Extracted Using Resnet50 Model.

Table [IV] presents the results of the three classifications using the KNN classifier along with the features extracted using the ResNet50 model. The table shows the accuracy, recall, and f1 score matrix for each chapter, as well as average values across all chapters and overall accuracy.

For the “Normal” category, the accuracy is 0.94, indicating that 94% of the samples classified as “Normal” were correctly identified. The recall is 0.92, which means that 92% of the actual “normal” samples were correctly labeled. The score of f1, which combines accuracy and recall, is 0.93 for the “normal” category.

Similarly, for the “viral pneumonia” category, the accuracy is 0.98, indicating that 98% of the samples classified as “viral pneumonia” were correct. The recall is 0.98, indicating that 98% of the actual “viral pneumonia” samples were correctly labeled. The f1 score for this category is also 0.98. Regarding the category “COVID-19”, the accuracy is 0.93, which means that 93% of the samples classified as “COVID-19” were correct. The recall is 0.95, indicating that 95% of actual “COVID-19” samples were correctly labeled. The f1 score for this category is 0.94. The average accuracy, recall, and f1 in all categories are 0.95, 0.95, and 0.95, respectively.

Finally, the overall accuracy of the KNN classifier along with the features extracted using the ResNet50 model was reported as 0.95, indicating that 95% of all samples were correctly classified in all categories.

TABLE IV: KNN CLASSIFIER RESULTS ALONG WITH FEATURES EXTRACTED USING THE RESNET50 MODEL.

• **ResNet50**			
• **Fitness**	[5] **Precision**	[6] **Recall**	[7] **F1 Score**
natural	0.94	0.92	0.93
Viral Pneumonia: 6	0.98	0.98	0.98
COVID-19	0.93	0.95	0.94
Moderate	0.95	0.95	0.95
Accuracy	Fig. 5. **0.95**		

4.1.2.2 Results of SVM Workbook with VGG16 Extracted Features:

Figure (7) below shows the confusion matrix for the KNN classifier application along with the features extracted using the VGG16 model on three categories: COVID-19, normal pneumonia, and viral pneumonia. The confusion matrix allows us to evaluate the performance of a workbook by comparing its predictions to actual labels.

Starting with the COVID-19 category, the classifier correctly identified 587 cases as COVID-19 (real positives), but mistakenly classified 17 cases as non-COVID-19 when they were actually COVID-19 (false negatives). In addition, the model incorrectly classified 3 cases as COVID-19 when they were not (false positives). This indicates that the classifier

had high accuracy in identifying COVID-19 cases, but had some cases where it failed to recognize the presence of COVID-19.
Moving into the normal category, the model accurately classified 465 cases as normal (real positives). However, it incorrectly predicted 108 cases as abnormal when they were already normal (false negatives). Furthermore, there were 37 instances where the classifier was incorrectly classified as normal when it was not (false positives). This suggests that although the model was generally adept at recognizing normal cases, it had difficulty identifying some cases correctly, resulting in both false negatives and false positives.
For the viral pneumonia category, the classifier showed strong performance. 555 cases were correctly identified as viral pneumonia (true positives) and only 7 cases were incorrectly classified as non-viral pneumonia (false negatives). Similarly, there were 3 cases where the classifier was incorrectly classified as viral pneumonia when it was not (false positives). Overall, the model showed high accuracy in identifying cases of viral pneumonia with minimal misclassifications.
In summary, the confusion matrix of the KNN classifier along with the features extracted using the VGG16 model demonstrates its efficacy in classifying cases of COVID-19 and viral pneumonia. However, there is room for improvement in accurately identifying normal states, as evidenced by high numbers of false negatives and false positives. These results provide valuable insights to further improve the model and enhance its overall performance in classifying chest X-ray images.

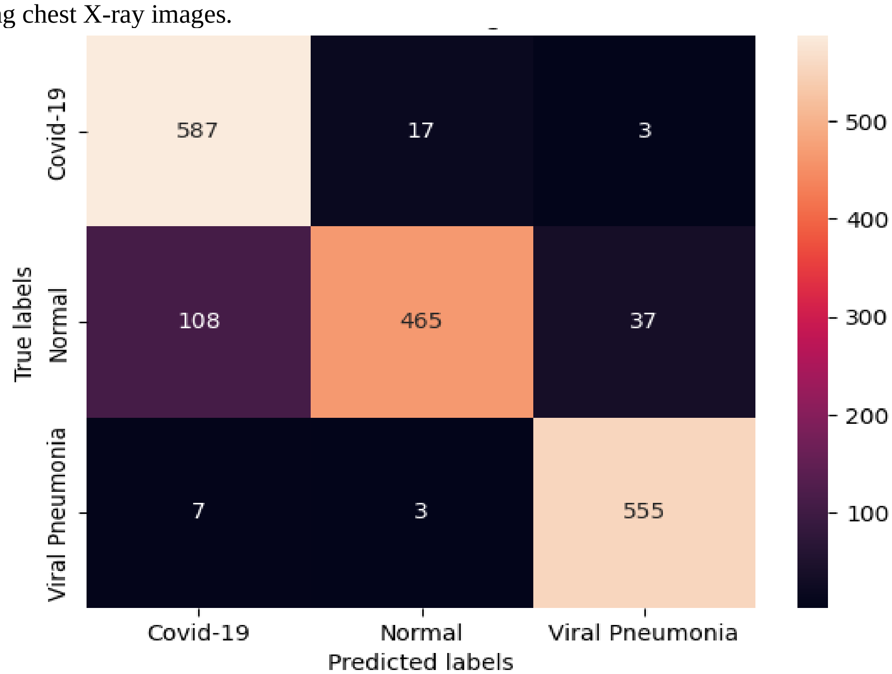

Fig 7: Confusion matrix ofKNN classifier with features extracted using VGG16 model.

Table [V] below presents the results of the three classifications using the KNN classifier along with the features extracted using the VGG16 model. The table shows the accuracy, recall, and f1 score matrix for each chapter, as well as average values across all chapters and overall accuracy.
In the context of the “Normal” category, rating scales provide important insights into the performance of a rating model. An accuracy score of 0.96 indicates that of the samples classified as “normal,” a high of 96% was correctly identified as such. This indicates a high level of accuracy in correctly classifying cases as' normal '.
On the other hand, a recall score of 0.74 reveals that the classifier was able to correctly capture 74% of the actual “normal” samples. This measure measures a classifier's ability to identify and include many true “normal” states in its classification.
For an overall rating, f1 combines accuracy and recall on a single scale. For the “Normal” category, the score for f1 is calculated as 0.84. This score takes into account both accuracy and recall values, providing a general measure of the effectiveness of the model in accurately classifying cases as “normal.”
The degree of accuracy indicates a low number of false positives, suggesting that the classifier has a strong ability to correctly identify cases as “normal.” However, the slightly lower recall score suggests that there may be some instances of the “normal” category being misclassified as something else. The f1 score provides a balanced assessment, taking into account both accuracy and recall, and serves as a useful measure to assess the overall performance of the model in classifying cases as' normal '.

Similarly, for the “viral pneumonia” category, the accuracy is 0.94, meaning that 94% of the samples classified as “viral pneumonia” were correct. The recall is 0.98, indicating that 98% of the actual “viral pneumonia” samples were correctly labeled. The f1 score for this category is also 0.98.
Regarding the category “COVID-19”, the accuracy is 0.93, which means that 93% of the samples classified as “COVID-19” were correct. The recall is 0.95, indicating that 95% of actual “COVID-19” samples were correctly labeled. The f1 score for this category is 0.94. The average accuracy, recall, and f1 in all categories are 0.95, 0.95, and 0.95, respectively. Finally, the overall accuracy of the KNN classifier along with the features extracted using the VGG16 model was 0.89, indicating that 89% of all samples were correctly classified in all categories.

TABLE V: KNN CLASSIFIER RESULTS ALONG WITH FEATURES EXTRACTED USING VGG16 MODEL.

• **KNN-VGG16**			
• **Fitness**	[8] **Precision**	[9] **Recall**	[10] **F1 Score**
natural	0.96	0.74	0.84
Viral Pneumonia: 6	0.94	0.98	0.84
COVID-19	0.81	0.96	0.88
Moderate	0.90	0.89	0.85
Accuracy	Fig. 6. **0.89**		

4.2 Multi-View Rating Results:

In this section, we present the results of the multi-view ranking approach used in our study. Specifically, we evaluate the accuracy achieved by the SVM and KNN classifiers when combining features extracted from the ResNet50 and VGG16 models, which were then combined using the early integration algorithm. Our analysis revealed promising results, with the SVM classifier achieving 98% accuracy when applied to built-in features. This indicates that the SVM classifier has successfully classified chest X-ray images into the respective categories with a high level of accuracy. Similarly, the KNN classifier achieved 92% accuracy when applied to built-in features, demonstrating its effectiveness in correctly identifying chest conditions.

4.2.1 Multi-observed SVM results using the early fusion approach:

Figure (8) shows the confusion matrix resulting from the application of a multi-viewed SVM classifier using an early fusion approach to three categories: normal viral pneumonia and COVID-19. The matrix provides a visual representation of a classifier's performance by showing the number of correctly and incorrectly classified samples within each category.
Starting with the “normal” category, the confusion matrix reveals that out of a total of 600 samples belonging to this category, 600 samples were accurately classified as normal. However, there were 10 cases in which samples from the normal category were mistakenly classified as viral pneumonia, and two samples were mistakenly classified as COVID-19.
Moving into the category “viral pneumonia”, the matrix shows that 578 samples were correctly classified as viral pneumonia out of a total of 593 samples from this category. However, there were 14 cases in which samples from other categories were incorrectly classified as viral pneumonia. In addition, one sample of the viral pneumonia category was incorrectly identified as COVID-19.
In the case of the “COVID-19” category, the confusion matrix indicates that out of 577 samples belonging to this category, 573 samples were correctly classified. However, three samples from other categories were mistakenly classified as COVID-19, and one sample from the COVID-19 category was mistakenly classified as viral pneumonia.
By examining the confusion matrix, we can gain insights into the workbook's performance across different categories. The multi-observed SVM classifier, applying the early fusion approach, clearly achieved a high level of accuracy in classifying normal samples. However, there were some mistaken classifications within the categories of viral pneumonia and COVID-19, as shown by values outside the diagonal line. Overall, the multi-observed SVM classifier, using the early fusion approach, demonstrates a commendable performance, as many samples were correctly classified across the three categories considered.

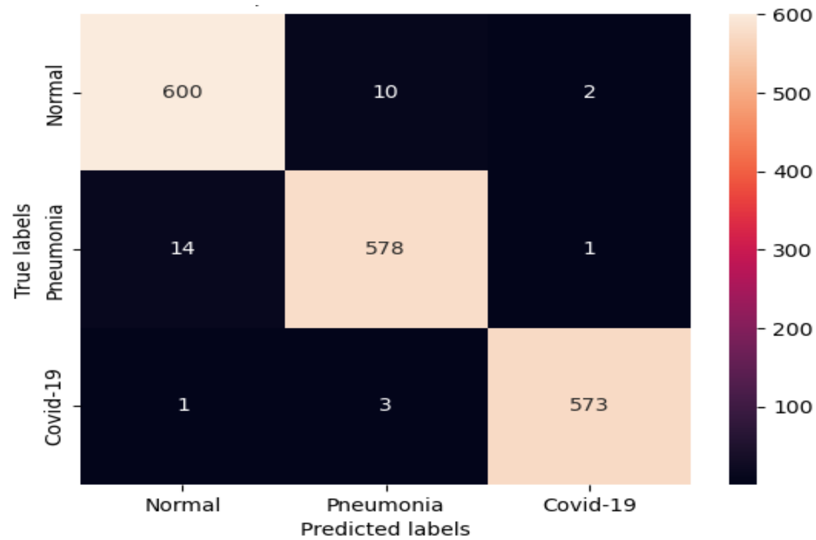

Fig 8: Confusion Matrix for Multi-View SVM Using the Early Fusion Approach.

Table [VI] presented presents the detailed results of an SVM workbook when combined with features combined using an early integration approach. Provides f1 accuracy, recall, and score scales for each class, along with average values across all classes.

For the “Normal” category, the SVM Multi-View classifier achieved an accuracy of 0.98, indicating that 98% of the samples classified as “Normal” were correctly classified. A recall value of 0.97 indicates that the workbook accurately identified 97% of the actual “normal” samples. The f1 score, which combines accuracy and recall, is 0.97, reflecting a balanced performance in terms of accuracy and recall for the “normal” category.

Similarly, for the category “viral pneumonia”, the SVM multiview classifier showed high accuracy and recall scores of 0.99. This means that the classifier performed exceptionally well in correctly identifying “viral pneumonia” samples. A f1 score of 0.99 also confirms the accuracy and effectiveness of the workbook in this particular category.

In the case of the category “COVID-19”, the SVM multiview classifier achieved an accuracy of 0.98, indicating a 98% accuracy in classifying samples as “COVID-19”. A recall value of 0.98 indicates that the classifier effectively identified 98% of actual COVID-19 samples. The f1 score of 0.97 reflects the overall performance of the classifier for this category.

Furthermore, the 'average' grade provides average accuracy, recall, and f1 score across all categories. In this case, the average accuracy and recall is 0.97, indicating consistent performance across all categories. These results demonstrate the overall effectiveness of a multi-viewed SVM workbook using an early integration approach.

By looking at the accuracy, recall, and f1 scales for each category, along with average values, we gain a thorough understanding of the workbook's performance. These results suggest that the SVM classifier, using features combined through an early integration approach, achieved high accuracy, accuracy, and recall for all three categories.

TABLE VI: MULTI-OBSERVED SVM RESULTS USING THE EARLY FUSION APPROACH.

• **Multi View**			
Fitness	Fig. 7. **Precisi on**	Fig. 8. **Re call**	Fig. 9. **F1 Score**
natural	0.98	0.97	0.97
Viral Pneumonia: 6	0.99	0.99	0.99
COVID-19	0.98	0.98	0.98
Moderate	Fig. 10. **0.98**	Fig. 11. **0.9 8**	Fig. 12. **0.98**
Accuracy	Fig. 13. **0.98**		

4.2.2 Kharafi National Multi-Vision Network Results Using Early Integration Approach:

Figure (9) shows the confusion matrix obtained from the application of the multiview KNN classifier using the early fusion approach to classify samples into three categories: normal pneumonia, viral pneumonia, and COVID-19.

Starting with the “normal” category, the confusion matrix reveals that out of a total of 600 samples belonging to this category, 600 samples were accurately classified as normal. However, there were 10 cases in which samples from the normal category were mistakenly classified as viral pneumonia, and two samples were mistakenly classified as COVID-19.

Moving into the category "viral pneumonia", the matrix shows that out of 609 samples from this category, 494 samples were correctly classified. However, there were 14 cases in which samples from other categories were incorrectly classified as viral pneumonia. In addition, one sample of the viral pneumonia category was incorrectly identified as COVID-19.

In the case of the "COVID-19" category, the confusion matrix indicates that out of 577 samples belonging to this category, 573 samples were correctly classified. However, three samples from other categories were mistakenly classified as COVID-19, and one sample from the COVID-19 category was mistakenly classified as viral pneumonia.

The confusion matrix analysis provides insights into the performance of the multi-viewed KNN classifier using an early integration approach across the three categories. The classifier achieved high accuracy in classifying normal samples, with the vast majority of them correctly identified. However, there were some mistaken classifications within the categories of viral pneumonia and COVID-19, as shown by values outside the diagonal line.

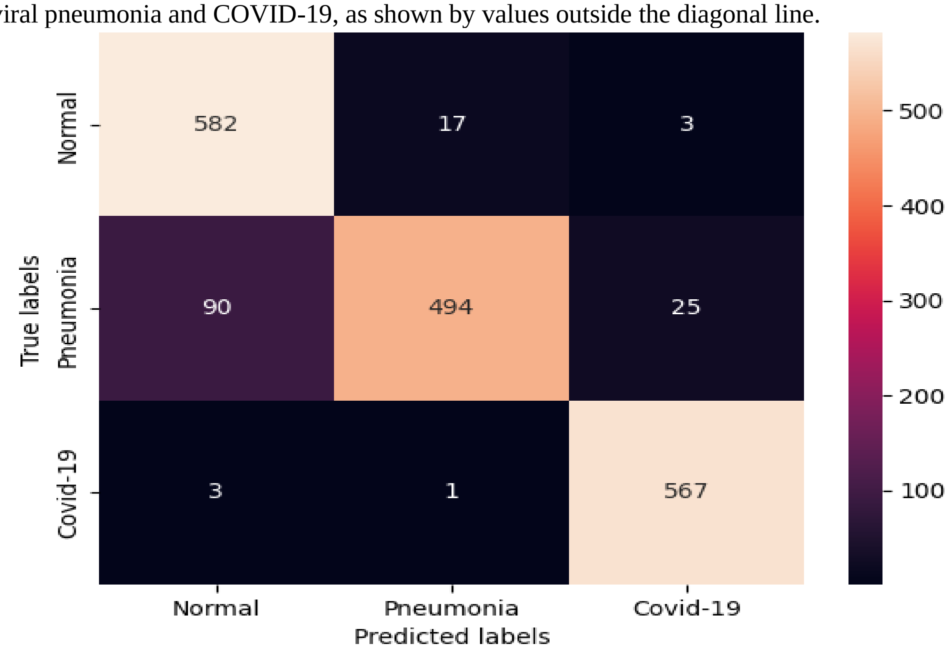

Fig 9: Multi-View National Knowledge Network Confusion Matrix Using Early Integration Approach.

Table [VII] presents the results of the three rankings using a multi-view KNN classifier using an early integration approach. The table shows the accuracy, recall, and f1 score matrix for each chapter, as well as average values across all chapters and overall accuracy.

Starting with the exact values for the normal viral pneumonia and COVID-19 categories, they are slightly lower compared to the multi-view SVM classifier, which ranges from 0.86 to 0.96. This suggests that the multi-viewed KNN classifier using the early integration approach has relatively less ability to accurately identify positive cases, especially for COVID-19. Transition to recall values for normal classes and COVID-19 classes is slightly lower compared to the multi-width SVM classifier, which ranges from 0.81 to 0.97.

However, the recall of the viral pneumonia category is higher (0.99). This suggests that the multi-observed KNN classifier has less ability to correctly identify true positive cases of viral pneumonia. Moreover, the f1 scores for all three categories are lower compared to the multi-view SVM classifier, which ranges from 0.88 to 0.97. Low f1 scores indicate relatively lower overall performance of a multi-view KNN classifier compared to a multi-view SVM classifier.

Finally, the overall accuracy of a multi-viewed KNN classifier using the early fusion approach is 0.92, indicating that it correctly classifies 92% of cases in the dataset, which is slightly lower compared to a multi-viewed SVM classifier.

In summary, the SVM multisentry classifier using the early fusion approach outperforms the KNN multisentry classifier in terms of accuracy, recall, f1 score, and accuracy for all three categories (normal viral pneumonia, COVID-19). The multi-view SVM classifier shows higher performance and better ability to classify cases accurately.

TABLE VII: MULTI-OBSERVED SVM RESULTS USING THE EARLY FUSION APPROACH.

• **Multi View**			
Fitness	Fig. 14. **Precision**	Fig. 15. **Recall**	Fig. 16. **F1 Score**
natural	0.96	0.81	0.88

Viral Pneumonia: 6	0.95	0.99	0.97
COVID-19	0.86	0.97	0.91
Moderate	0.92	0.92	0.92
Accuracy	Fig. 17. **0.92**		

4.3 Discuss the results of all models:

In this section, a comparative analysis was carried out to examine the performance of the different models used through this letter. Figure (10) shows that the adoption of multi-observed SVM using the early integration approach achieved the highest degree of accuracy, recall, and f1. These results provide strong evidence that SVM outperforms other models in the context of multi-view ranking. By minimizing false positive predictions, a multi-viewed proprietary value management approach shows higher accuracy, reducing the incidence of false alarms and unnecessary interventions. In addition, a high recall score indicates greater accuracy in detecting positive cases. On the other hand, the VGG16 model with KNN shows the lowest values for accuracy, recall, and f1, indicating its relative inefficiency compared to other models.

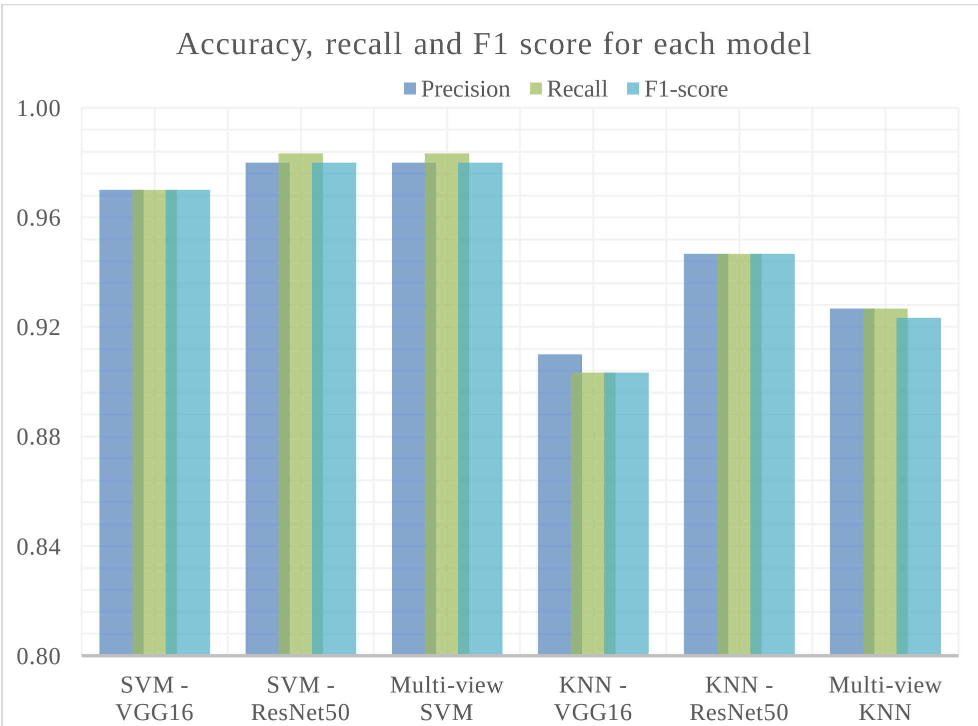

Fig 10: Accuracy, recall, and F1 score for each model.

The relationship between f1 score and accuracy is influenced by the class distribution and the specific characteristics of the classification problem. In cases where the class distribution is balanced and all categories are equally important, the score of f1 and accuracy tend to be similar or closely related. Therefore, in our scenarios where high accuracy is achieved, it generally corresponds to a high f1 score, and vice versa. This can be seen in Figures (11, 13and 14) of our results. In addition, in Figure 11, when RiseNet50 is used to extract features with an SVM classifier, it outperforms the KNN approach.

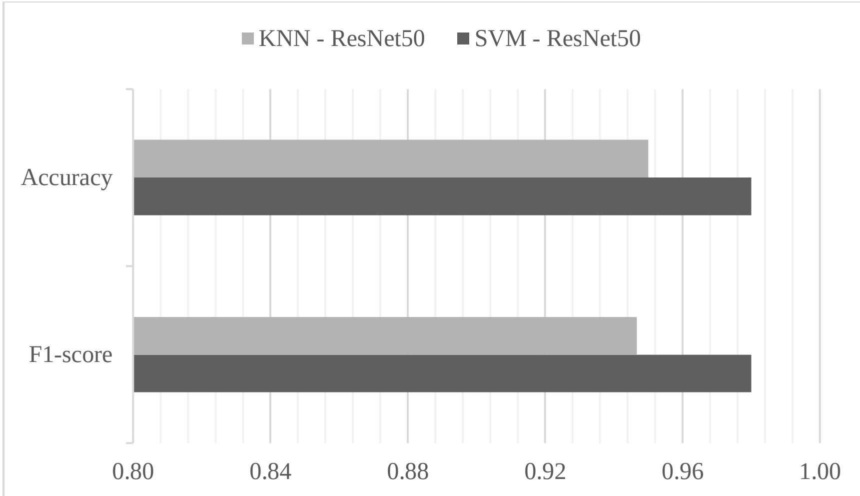

Fig 11: SVM vs. KNN classifiers combined with features extracted using ResNet50 model.

Furthermore, Figure (12) shows that the performance of the KNN classifier, when combined with the features extracted with the VGG16 model, is less efficient compared to the SVM classifier. The f1 score in KNN does not come close to the level of accuracy compared to other models, and this observation is consistent with the results in Figure (12), where the accuracy, recall and f1 score of the KNN model indicate that it is less effective in detecting and predicting cases of COVID-19 and viral pneumonia compared to normal conditions.

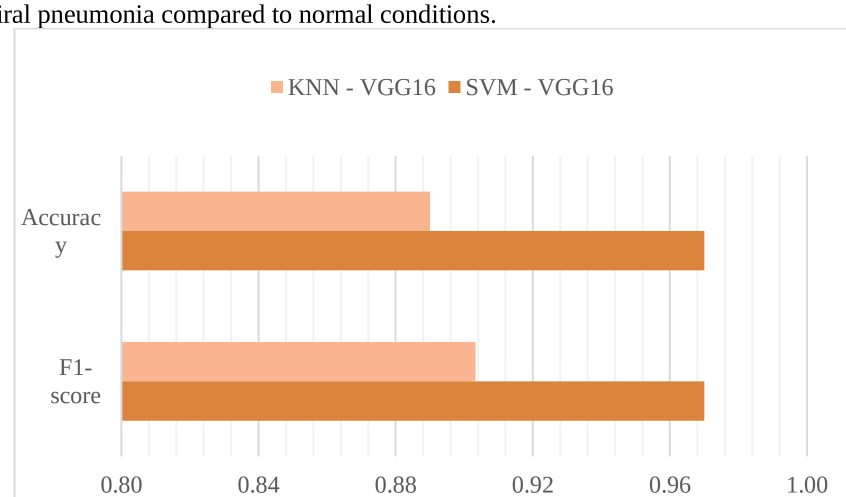

Fig 12: SVM vs. KNN classifiers combined with features extracted from VGG16.

Furthermore, in FIG. 15, it can be seen that the SVM classifier outperforms the KNN classifier in multi-display classification. The f1 score of both models can be considered a reliable measure. As mentioned in the discussion of Figure (13), the multi-view SVM classifier using early fusion achieves the highest accuracy among all models. This score is consistent with accuracy, recall, and f1 scores, further highlighting the superior performance of a multi-observed SVM classifier in a classification task.

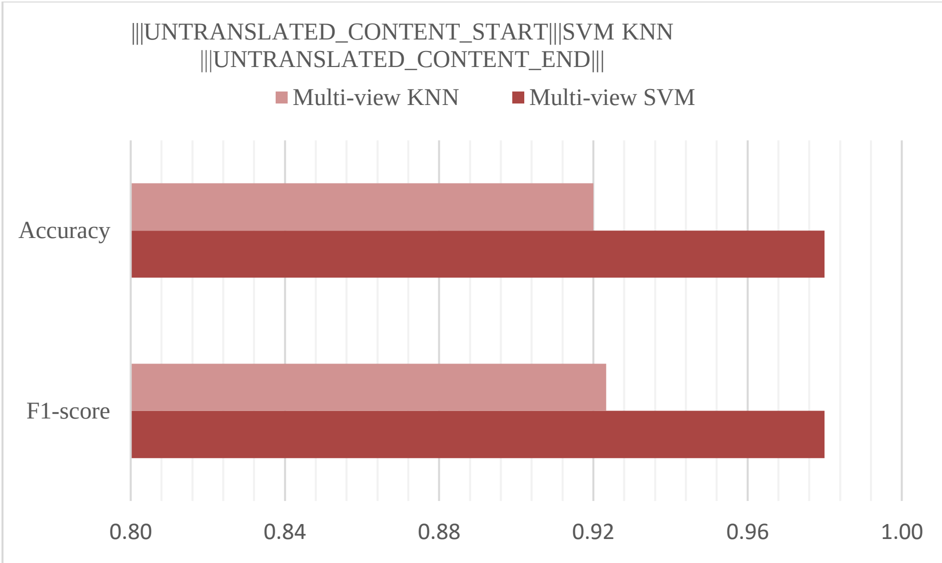

Fig 13: SVM versus KNN using the early fusion approach.

As shown in Figure (14), the use of an SVM classifier with multi-display data shows little improvement compared to its use with a single data display (RezNet50 and VGG16). This observation indicates the high efficacy of the SVM classifier in general for the detection of COVID-19 and viral pneumonia from normal conditions in chest X-ray images. It should be noted that all rating scales achieved values above 96%, highlighting the strong performance of the SVM rating on this task.

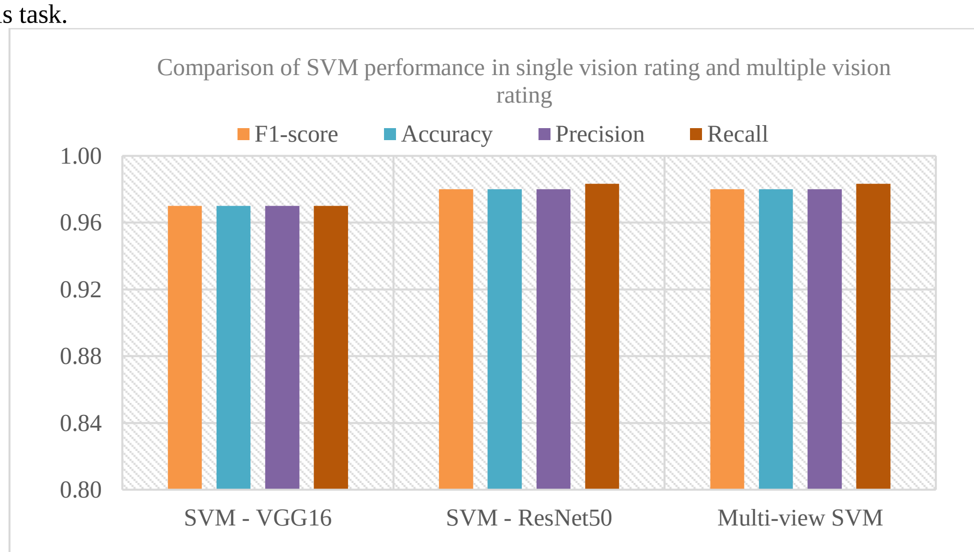

Fig 14: Comparison of SVM performance in single view rating and multiple view rating.

From fig. 15, it can be seen that the accuracy and performance of KNN were significantly higher when using ResNet50 compared to VGG16 in the single view rating. Furthermore, the use of multi-view rating showed an improvement over KNN when applied with VGG16, while it showed lower performance compared to KNN when applied with ResNet50.

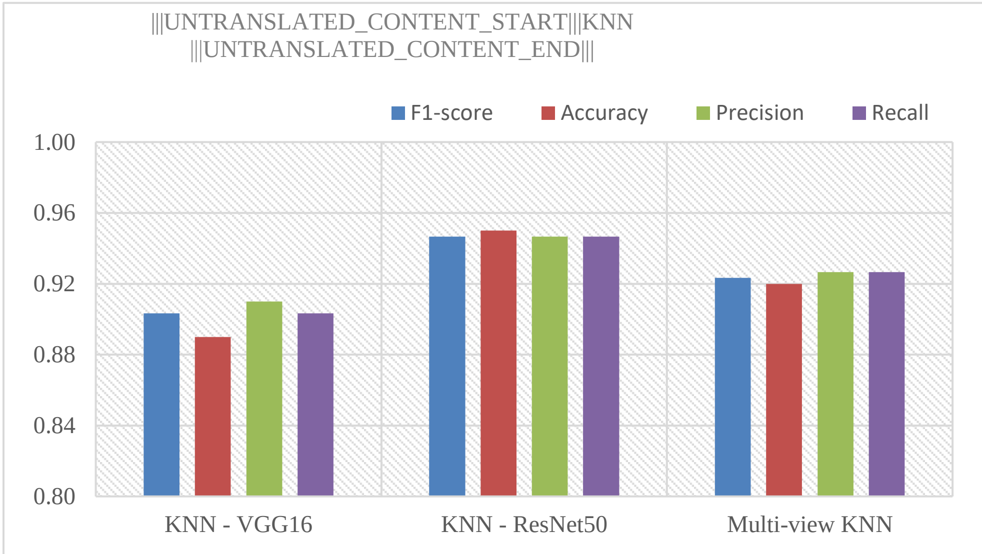

Fig 15: Comparison of KNN's performance in single view and multiple view ranking.

Funding:

The authors confirm that no funding was acquired from any organization, grant agency, or institution. This research was undertaken without any external financial contributions.

Conflicts of Interest:

The authors declare no competing financial interests in this study.

Acknowledgment:

The authors would like to thank their institutions for providing the necessary facilities and guidance, which proved vital in achieving the study's objectives.

References

[1] WHO EMRO, "Questions and answers: COVID-19," Health Topics. [Online]. Available: https://www.emro.who.int.
[2] A. Al-Hazmi, "Challenges presented by MERS corona virus and SARS corona virus to global health," Saudi Journal of Biological Sciences, vol. 23, no. 4, pp. 507–511, 2016.
[3] WHO, "Coronavirus Disease (COVID-19) - events as they happen." [Online]. Available: https://www.who.int.
[4] Z. Wu and J. M. McGoogan, "Characteristics of and important lessons from the coronavirus disease 2019 (COVID-19) outbreak in China: summary of a report of 72,314 cases from the Chinese Center for Disease Control and Prevention," JAMA, vol. 323, no. 13, pp. 1239–1242, 2020.
[5] WHO, "Director-General's remarks at the media briefing on 2019-nCoV on 11 February 2020." [Online]. Available: https://www.who.int.
[6] D. W. Bates, S. Saria, L. Ohno-Machado, A. Shah, and G. Escobar, "Big data in health care: using analytics to identify and manage high-risk and high-cost patients," Health Affairs, vol. 33, no. 7, pp. 1123–1131, 2014.
[7] J. Wiens and E. S. Shenoy, "Machine learning for healthcare: on the verge of a major shift in healthcare epidemiology," Clinical Infectious Diseases, vol. 66, no. 1, pp. 149–153, 2018.
[8] WHO, "COVID-19 situation reports." [Online]. Available: https://www.who.int.
[9] Worldometer, "Countries where coronavirus has spread." [Online]. Available: https://www.worldometers.info.
[10] T. Chowdhury et al., "Can AI help in screening Viral and COVID-19 pneumonia?" IEEE Access, vol. 8, pp. 132665–132676, 2020. [Online]. Available: https://www.kaggle.com/tawsifurrahman/covid19-radiography-database.
[11] P. Mooney, "Chest X-Ray Images (Pneumonia)," [Online]. Available: https://www.kaggle.com/datasets/paultimothymooney/chest-xray-pneumonia.
[12] R. Mohammad and A. Abolfazl, "A new modified deep convolutional neural network for detecting COVID-19 from X-ray images," arXiv preprint, arXiv:2004.08052, 2020.
[13] H. M. Saleh, M. H. Marouane, and A. Fakhfakh, "Improves intrusion detection performance in wireless sensor networks through machine learning, enhanced by an accelerated deep learning model with advanced feature selection," Iraqi Journal for Computer Science and Mathematics, vol. 5, no. 3, pp. 23, 2024.
[14] K. A. Tait, J. S. Khan, F. Alqahtani, A. A. Shah, F. A. Khan, M. U. Rehman, et al., "Intrusion detection using machine learning techniques: an experimental comparison," in 2021 International Congress of Advanced Technology and Engineering (ICOTEN), pp. 1–10, Jul. 2021.